Journal of Inclusion Phenomena **5** (1987), 385–395.

ESR Spectroscopic Study and Kinetic Discussion of the Disproportionation Reaction of Nitrogen Monoxide on CaHY-type Zeolite

Y. KANNO★
Government Industrial Research Institute, Nagoya, Hirate-cho, Kitaku, Nagoya 462, Japan

Y. MATSUI★★ and H. IMAI
Research Laboratory of Engineering Materials, Tokyo Institute of Technology, Nagatsuta-cho, Midiri-ku, Yokohama 227, Japan

(Received: 27 August 1986)

Abstract. An ESR spectroscopic study of adsorbed NO on CaHY-type zeolite was carried out and the kinetics are discussed on the basis of a mechanistic model of the disproportionation reaction. An amount of NO less than the amount of Ca^{2+} distributed in Site II of the faujasite structure was admitted onto the sample maintained at 373 K. ESR spectra were recorded at room temperature. The spectra consisted of well-resolved signals. It is proposed that NO molecules on CaHY-type zeolite have two kinds of adsorption patterns. The initial formation of N_2O may be expressed by the following reactions:

$$[\ \ ] + NO \overset{K_1}{\rightleftharpoons} [NO],\ [NO] + NO \underset{\overleftarrow{k_2}}{\overset{\vec{k_2}}{\rightleftarrows}} [N_2O_2],\ [N_2O_2] + NO \overset{\vec{k_3}}{\rightarrow} [NO_2] + N_2O\ ,$$

where [ ], [NO] and $[N_2O_2]$ denote vacant adsorption, NO adsorption, and N_2O_2 adsorption sites, respectively. A rate equation for N_2O appearance (α) has been derived by a steady state approximation:

$$\alpha = \frac{\vec{k}_3 K_1 K_2 P^3}{1 + (K_1 + \vec{k}_3/\overleftarrow{k}_2)P + K_1(K_2 + \vec{k}_3/\overleftarrow{k}_2)P^2}\ ,$$

where P is the pressure of NO. The rate equation was used to explain the kinetic results of the disproportionation of NO.

Key words: Nitrogen monoxide, ESR spectroscopy, disproportionation reaction, CaHY-type zeolite, kinetics.

1. Introduction

The ESR spectrum of adsorbed NO molecules was used to investigate the crystal field interactions on the surface of zeolites [1–4]. These studies suggested that the NO molecule is an important probe for understanding the properties of active catalytic sites inside zeolites. In a dynamic study of the ESR spectrum of the adsorbed NO molecules on the alkaline-earth Y-type zeolites, which were measured at liquid nitrogen temperature, Lunsford reported that as one moved up the series from BaY- to MgY-type zeolites, the three-line hyperfine showed less resolution. This loss in resolution was possibly ascribed to the presence of a second broad peak [5].

★ Author for correspondence.
★★ Present address: Asahi Diamond Co., Kuji, Takatsu-ku, Kawasaki 213, Japan.

In the study of the sorption and reactivity of NO, Addison and Barrer [6] found that the disproportionation reaction of NO ($4\,NO \rightleftharpoons N_2O + N_2O_3$) occurred on chabazite, faujasite, and A-type zeolites at 273 K or lower temperatures. Later, an infrared spectroscopic study for the disproportionation reaction of NO at room temperature was reported and the reaction mechanism was discussed [7, 8]. Kasai and Bishop studied the ESR spectra of NO adsorbed on NaY-, ZnY-, and BaY-type zeolites [9]. They proposed that N_2O_3 formed by the disproportionation reaction was ionized to yield NO^+ and NO_2^-, and that a proper redistribution of these cations and anions resulted in the uniformity of the crystal field.

Recently we studied the disproportionation reaction of NO on various Y-type zeolites and alkaline-earth oxides at near room temperature [10–15]. We proposed that the active sites for this reaction were metal ions located in Site II of the faujasite structure, and the reaction sequence was determined. ESR experiments on NO adsorption on the alkaline-earth Y-type zeolites were formerly done at 77 K. It is very important to measure ESR spectra at room temperature because the investigation of sorption and reactivity of NO (i.e., the disproportionation reaction) was carried out at room temperature.

The understanding of the reactivity of NO is also of great interest in studies related to the transformation and elimination of atmospheric pollutants. In the present work, we report the ESR spectra of adsorbed NO molecules on the CaHY-type zeolite, which were measured at room temperature, and a kinetic discussion based on the mechanistic model of disproportionation of NO.

2. Experimental

Nitrogen monoxide and carbon monoxide, the nominal purities of which were 99.0% and 99.5%, respectively, were obtained from Takachiho Chemical Industry Ltd. and used without further purification. A NaY-type zeolite (Union Carbide Co.) was ion-exchanged 16 times at 90 °C with a 10% solution of ammonium nitrate, and the resultant NH_4Y-type zeolite was further ion-exchanged with a solution of calcium nitrate. The composition of the resultant $CaNH_4Y$-type zeolite corresponds to $Ca_{24.0}(NH_4)_{8.0}Na(AlO_2)_{57}(SiO_2)_{135} \cdot nH_2O$ per unit cell (degree of exchange *ca.* 86%). Chemical analysis of the sample was done by flame spectrophotometry and atomic absorption spectrophotometry. The $CaNH_4Y$-type zeolite was washed three times with 0.1 N calcium nitrate solution and dried overnight at 110 °C. This sample was pressed and ground into pieces of 32 to 60 mesh. The powder X-ray diffraction pattern confirmed that no structural damage was produced during the sample preparation. Before the spectrum measurement, the CaHY-type zeolite was prepared by ammonia removal of the $CaNH_4Y$-type zeolite. After the treatment at 423 K for 3 h in a stream of dry air, the temperature of the sample weighing *ca.* 10 g was increased to 973 K [16] at a constant rate of 0.5 K/min. The sample was then kept constant for 4 h at 973 K, and evacuated (10^{-6} Torr) at the same temperature for 2 h in an ESR sample tube. The desired amount of NO was admitted onto the sample. A conventional X-band ESR spectrometer (JEOL FE1X) with a TE_{102} mode cavity was employed. Determination of the g-values and spin concentrations was done with 2,2-DPPH and $CuSO_4 \cdot 5H_2O$, respectively. The adsorption of CO was measured at 0 °C in the pressure range 0–200 Torr by means of a volumetric method [17]. The pretreatment in the CO adsorption experiment was similar to that of the ESR experiment.

The measurement of catalytic activity was performed by a pulsed microreactor. The pretreatment of the catalyst was done in a similar fashion to that of the ESR experiment. A temperature programmed desorption (TPD) study was carried out. After a run of the pulsed

reaction, the temperature of the sample was raised at a constant rate of 7.14 °C/min in a stream of He carrier gas and the amount of desorbed gas was recorded by a TCD detector. The NO_2 component contained in the effluent gas was removed by a dry NaOH/silica column before entering the TCD detector.

3. Results and Discussion

3.1. ESR SPECTRA OF ADSORBED NO

Figure 1(a) shows the spectrum recorded at room temperature, where NO was admitted onto the samples at room temperature and at a pressure of 10 Torr. The spectrum is very weak. Figure 1(b) shows the spectrum recorded at 77 K on the sample in Figure 1(a). The spectrum in Figure 1(b) can be removed by evacuation at room temperature for 10 min.

Rabo *et al.* [18, 19] examined the IR spectra of CO adsorbed on faujasite, and suggested that the chemisorption of CO served as an indicator of accessible divalent cations in the zeolite. Egerton and Stones [20, 21] studied the adsorption of CO on the Y-type zeolites exchanged with various metal ions and concluded that CO was chemisorbed on the metal ions

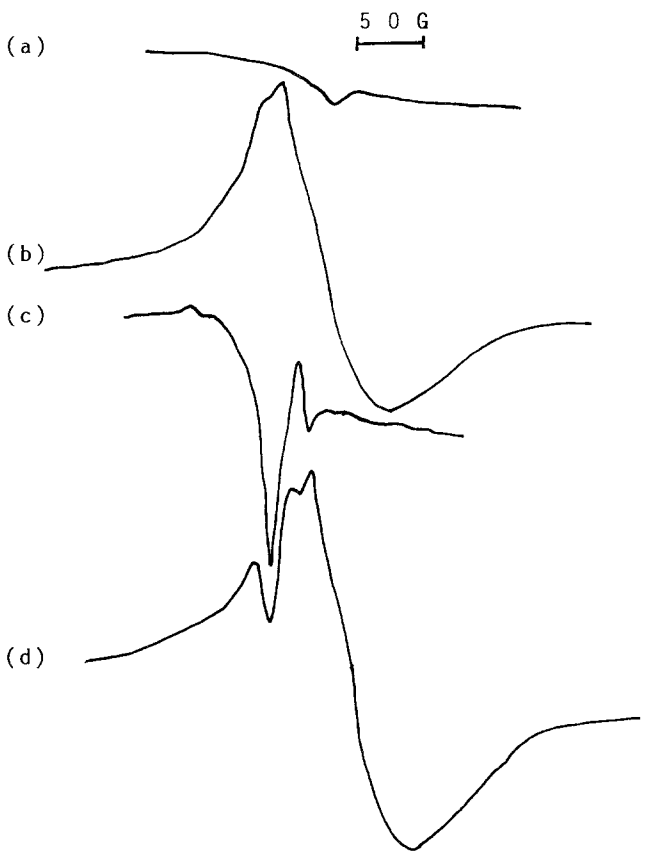

Fig. 1. ESR spectra of NO adsorbed onCaHY-type zeolite: (a) 10 Torr NO was admitted at RT, recorded at RT, (b) 10 Torr NO was admitted at RT, recorded at 77 K, (c) NO (6.49×10^{-5} mol/g) was admitted at 373 K, recorded at RT, (d) NO (6.49×10^{-5} mol/g) was admitted at 373 K, recorded at 77 K.

occupying Site II. We reported formerly that the active sites for the disproportionation reaction of NO were cations located in Site II [22] of the faujasite structure [10, 11], and concluded that the amount of Ca(II) could be determined from the chemisorption of CO [23]. (Here, Ca(II) indicates the amount of Ca^{2+} distributed in Site II.) The CO adsorption experiment showed that the amount of Ca(II) is 7.67×10^{-4} g-atom/g-catalyst in this work.

Lunsford reported a broad and ill defined signal on CaY-type zeolite [5], which was different from the well resolved signal detected from the adsorbed NO on MgO [24]. Kasai and Bishop reported that the spectrum on BaY-type zeolite became sharp and well-defined on standing at room temperature for several days [9]. They stated that this sharpening of the signal implied improved uniformity in the crystal field to which the NO molecules responsible for the ESR signal were subjected. However, no sharp spectra on CaY-type zeolite have been reported. In our study, a negative value for the activation energy in the disproportionation reaction of NO on CaY-type zeolite was found [10]. The dependence of the initial formation rate of N_2O on NO pressure was investigated with a gas circulation system. The rate of initial formation of N_2O was third order in NO pressure in lower pressure regions (*ca.* 30 Torr) [15]. This kinetic information and the work of Kasai *et al.* [9] prompted us to measure the ESR spectrum under strictly controlled conditions for the disproportionation reaction of NO. Control of this reaction can be attained by keeping the sample tube not at room temperature but at 373 K, and by admitting an amount of NO less than the Ca(II), without permitting the successive surface reaction of NO in the gas phase with Ca^{2+} in Site II (*cf.* reference 14 or Figure 4 in this paper).

In the following experiments, NO was admitted at 373 K. Figure 1(c) shows the ESR spectrum recorded at room temperature, where the amount of NO admitted into the sample tube corresponds to ca. one-tenth of Ca(II) (6.49×10^{-5} mol/g). It is particularly interesting to note that the introduction of a extremely small amount of NO (less than that of Ca(II)) gave the strong and well-resolved signal which was observed at room temperature. Furthermore, the spectrum observed at room temperature varied gradually with an increase of adsorbed molecules. Figure 1(d) shows the spectrum recorded at 77 K on the sample of Figure 1(c). The spectrum is the overlapping one of both the broad peak of Figure 1(b) and the well-resolved peak of Figure 1(c).

It is of interest to study the variation of ESR spectra with an increase of adsorbed NO. Figure 2(b), (c) and (d) show the spectra recorded at room temperature, where the amount of added NO is 1.55×10^{-4}, 3.90×10^{-4}, and 2.29×10^{-3} molecules/g, respectively. The spectrum in Figure 2(a), where added NO is *ca.* one-tenth of Ca(II), is characterized by $g_\perp = 2.016$, and $g_\parallel = 2.054$ (this signal is (A) in this paper). The g-values in signal (A) were larger than the g_e-value. We feel that these larger values were caused by the increase in orbital angular momentum effected by the d-orbitals of calcium. The nitrogen hyperfine coupling constant in signal (A) was so small that we could not resolve it at room temperature. In Figure 2(b), added NO being one-fifth of Ca(II), an overlapping spectrum of both signal (A) and a new peak was observed. Signal (A) vanished in Figure 2(c), where added NO is *ca.* one-half of Ca(II). A new signal, (B), characterized by $g_\perp = 2.004$, $g_\parallel = 1.989$, and $a_\perp = 27.0$ G for the N hyperfine splitting was detected. The spin concentrations of signal (A) and (B) were *ca.* 1.24×10^{17} and 2.6×10^{16} spins/g, respectively.

The intensity of signal (A) decreases in the early stages of adsorption, so we can estimate that the species producing (A) is more reactive than that causing (B). This may mean that signal (A) is affected by the disproportionation reaction. However, the intensity of signal (B) decreases more slowly; it is assumed that the adsorbed species begins to desorb slowly. This is easily deduced from the decrease of signal intensity shown in Figure 2(d), where added NO is three times that of Ca(II).

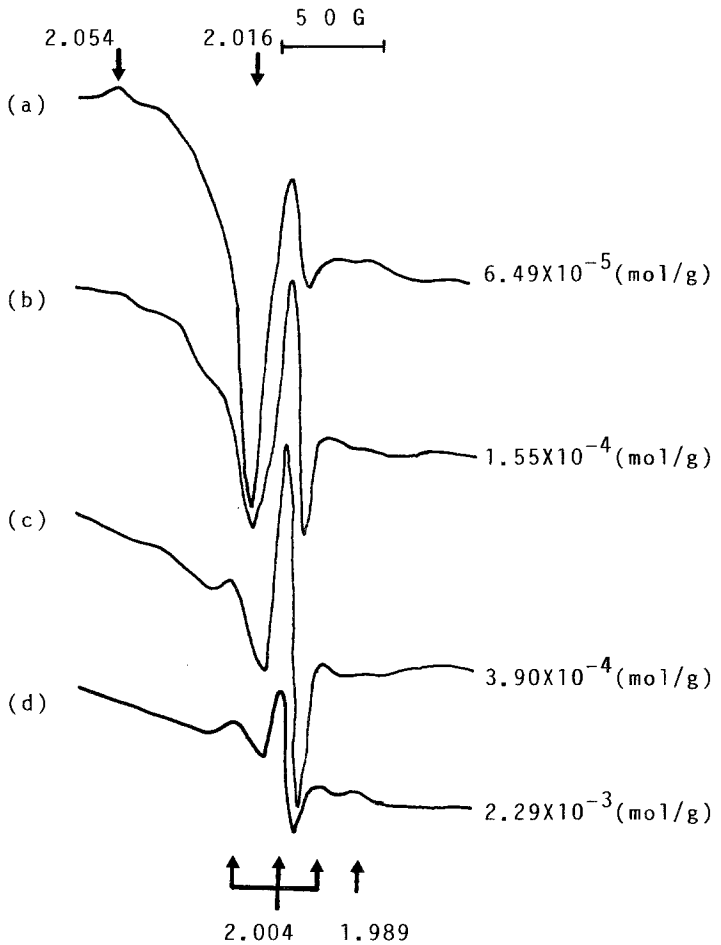

Fig. 2. Changes in the spectra as the adsorbed NO is increased, NO was admitted at 373 K and the spectra were recorded at RT.

We now consider the reason for two kinds of signals, (A) and (B). Comparison of Figure 1(c) with (d), shows that these two signals are not generated by the difference of the state of motion of NO molecules. Wasserman *et al.*, on the other hand, studied the theoretical ESR absorption spectrum for a randomly oriented triplet system for given values of D', E' and v. They reported the theoretical spectrum caused by the spin-spin interaction [25]. The theoretical spectrum is quite different from that of Figure 2. The two kinds of signals which appeared with an increase of the amount of adsorption may arise from two kinds of adsorption species having different hyperfine coupling constants. The g-value and the hyperfine coupling constants of signal (A) and (B) are summarized in Table I. Table I also shows the adsorption models (a), (b) and (c) derived from these values. The adsorption models will be discussed as follows:

(1) *model* (a) 'Ca^+NO^+'. Since calcium lacks d-electrons, it is unreasonable to consider that back donation occurs.

Table I. g-Tensors, hyperfine coupling tensors, and adsorption model of NO on CaHY-type zeolite

Signal	A	B
g_x	–	2.004
g_y	2.054	2.004
g_z	2.016	1.989
a_x	~0	~0
a_y	<8	27.0
a_z	~0	~0
Model (a)	Ca^+NO^+	$Ca^{2+}NO$
(b)	Ca^+NO^+	$Ca^+[^{NO}_{NO}]^+$
(c)	$Ca^{2+}NO$	$Ca^{2+}ON$

(2) *model* (b) '$Ca^+[^{NO}_{NO}]^+$'. We would have a hyperfine structure composed of five lines under the assumption, so the model is inappropriate. Therefore, model (c) is justified. It is reasonable to regard that signal (A) is ascribed to $Ca^{2+}NO$ and signal (B) is $Ca^{2+}ON$. From the variation of each signal intensity, it is estimated that the $Ca^{2+}NO$ species contribute to the progress of disproportionation of NO and then vanish in the earlier stage of adsorption. The $Ca^{2+}ON$ species, on the other hand, have no relation to the disproportionation and a decrease of signal intensity occurs more slowly. In the adsorption on the catalyst surface, NO molecules generally tend to adsorb with the arrangement that an atom having the stronger p-electron character is attached. This arrangement is satisfied if the N atom is 'on-top'. Therefore, the adsorption species $Ca^{2+}NO$ is seen to appear in the initial stage of adsorption.

Lunsford reported that the crystal-field splitting of the π^* levels (Δ) was *ca.* 0.2 eV [5]. In the present study, Δ was calculated to be *ca.* 2.3 eV. This suggests that a very strong crystal field is attained, and the strong crystal field leads to the well-resolved ESR spectrum measured at room temperature. In general, we note that in order to keep the strong crystal field within the zeolite structure: (1) rapid ion-exchange and a rapid temperature increase in the pretreatment of synthetic zeolites should be avoided. (2) the crystallinity of prepared zeolites should be checked by X-ray diffractometry or other techniques.

The present work suggests that one can get a well-resolved ESR signal of adsorbed NO by admitting a bit less NO than Ca(II) onto the sample maintained at 373 K. This means that the uniformity of the crystal field is attained by offering strict reaction conditions for the progress of the disproportionation of NO.

3.2. DISPROPORTIONATION REACTION OF NO

The catalytic activity was measured at 15°C. Strictly speaking, the disproportionation reaction of NO on a zeolite is not a catalytic reaction. The reaction is actually catalyzed by metal ions distributed in Site II of the faujasite structure [11]. Therefore, in this paper, the term catalytic activity is used from the viewpoint of catalytic action of active sites. The catalytic activity is conveniently defined as the formation rate of N_2O produced by the disproportionation within the first pulse. The relation between catalytic activity and pretreatment temperature in the range 400–900°C is shown in Figure 3. Furthermore, the TPD spectrum of CaY-type zeolite pretreated at 700°C is shown in an inner part of Figure 3. The

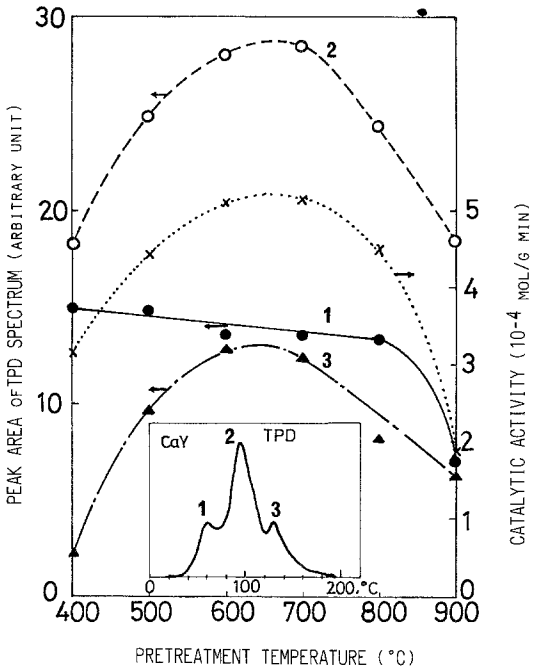

Fig. 3. Peak area of TPD spectrum and catalytic activity plotted against pretreatment temperature.

spectrum is composed of three peaks. The spectra of zeolites treated at a given pretreatment temperature are also composed of three peaks and the size of each peak varies independently of the others with regard to the pretreatment temperature. The TPD spectrum is divided into three peaks by drawing a supplementary line, and the relation between the area of each peak (1 : 2 : 3) and the pretreatment temperature are also shown in Figure 3. An analysis of desorbed gases showed that the first and second peaks were mainly composed of NO with the residual portion as N_2O, and most portion of the third peak was N_2O with the rest as NO.

3.3. DERIVATION OF RATE EQUATION

A mechanistic model of the disproportionation reaction of NO on CaHY-type zeolite was deduced from a previous infrared study [14], in which an eight-step model was proposed. The model is shown in Figure 4.

In the first step, (1), NO molecules interact with a positively charged Ca^{2+} and thus NO molecules adsorb on a Ca^{2+} site. In step (2), the chemisorbed NO species interact with NO in the gas phase, and the adsorbed N_2O_2 dimers are seen to form on the zeolite surface in step (3). The life-time of the adsorbed N_2O_2 dimers on the Ca^{2+} site is short, because we could not find any peaks to assign to it. The adsorbed N_2O_2 species interact with NO molecules of the gas phase, and the NO_2^+ species and N_2O are formed in step (4). The N_2O desorb into the gas phase, whereas the remaining NO_2^+ interacts with NO molecules and the adsorbed N_2O_3 species are produced in step (5).

A rate equation for the initial formation of N_2O was derived as follows by a steady-state approximation from this model, in which it was assumed that the reverse reaction of step

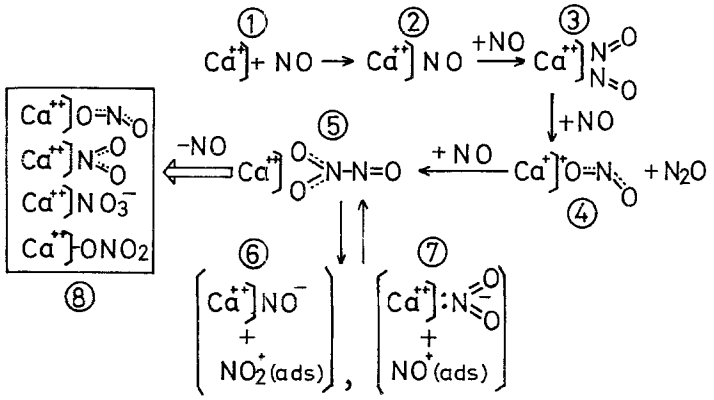

Fig. 4. Mechanistic model of the disproportionation reaction of NO on CaHY zeolite.

③ – ④ was negligible. On this assumption, we have the following reaction sequence for the initial formation of N_2O:

$$[\quad] + NO \overset{K_1}{\rightleftharpoons} [NO] \tag{1}$$

$$[NO] + NO \underset{\overleftarrow{k_2}}{\overset{\overrightarrow{k_2}}{\rightleftarrows}} [N_2O_2] \tag{2}$$

$$[N_2O_2] + NO \xrightarrow{\overrightarrow{k_3}} NO_2] + N_2O \tag{3},$$

where [ ], [NO], and $[N_2O_2]$ denote vacant adsorption sites, NO adsorption sites, N_2O_2 adsorption sites, respectively. K_1 is the equilibrium constant of Equation (1), and $\overrightarrow{k_2}$, $\overleftarrow{k_2}$, $\overrightarrow{k_3}$ are the rate constants of the respective reaction equations. The steady state approximation affords the next two equations:

$$d[N_2O_2]/dt = \overrightarrow{k_2}[NO]P - \overleftarrow{k_2}[N_2O_2] - \overrightarrow{k_3}[N_2O_2]P = 0 \tag{4}$$

$$[\quad] + [NO] + [N_2O_2] = 1\,. \tag{5}$$

An initial rate of formation of N_2O (α) is then formulated from Equation (1)–(5).

$$\alpha = \overrightarrow{k_3}[N_2O_2]P$$

$$= \frac{\overrightarrow{k_3}K_1K_2P^3}{1 + (K_1 + \overrightarrow{k_3}/\overleftarrow{k_2})P + K_1(K_2 + \overrightarrow{k_3}/\overleftarrow{k_2})P^2}\,, \tag{6}$$

where P is the pressure of NO and K_2 is k_2/k_2.

3.4. INVESTIGATIONS OF THE RATE EQUATION

In a kinetic study done with a closed gas circulation system, it was found that the reaction order for the formation of N_2O is proportional to the third order of NO gas pressure (P_0) in the lower pressure region (*ca.* 30 Torr). In an intermediate pressure region, the order of the initial rate gradually decreased with an increase of P_0 and obeyed the 2.2th order of P_0 in the higher pressure region (*ca.* 200 Torr) [15].

In order to investigate the kinetics of the disproportionation reaction of NO, we discuss the rate equation derived from the rate determining approximation. The experimental fact that

the rate of the initial formation of N_2O is proportional to the third order of NO pressure prompted us to note that the rate determining step is not the elementary steps (2) and (3), but step (3) – (4) in the mechanistic model of Figure 4. If Equation (3) is rate determining, Equation (2) is replaced by the following reaction:

$$[NO] + NO \overset{K_2}{\rightleftharpoons} [N_2O_2] . \tag{7}$$

Then, α is calculated from Equations (1), (3), (5), and (7):

$$\alpha = \frac{\vec{k}_3 K_1 K_2 P^3}{1 + K_1 P + K_1 K_2 P^2} . \tag{8}$$

If $\vec{k}_3$ is negligibly small compared to $\overleftarrow{k}_2$, i.e., $\vec{k}_3$ is rate determining, Equation (6) undoubtedly coincides with Equation (8).

The reaction order (n) is given by

$$\begin{aligned} n &= \partial \ln \alpha / \partial \ln P \\ &= 3 - K_1 P(1 + 2K_2 P)/(1 + K_1 P + K_1 K_2 P^2) \end{aligned} \tag{9}$$

Equation (9) shows that the initial rate of formation of N_2O is expected to obey a third-order relation with respect to NO pressure in the lower pressure region if K_1 is negligible small, and the order gradually decreases with an increase of pressure. At high NO pressure, the order approaches one. Thus, the rate equation explains the experimental facts obtained in a closed gas circulation system.

We previously reported that the apparent activation energies for the disproportionation of NO were – 6.9 Kcal/mol (CaY-type zeolite), and – 0.73 Kcal/mol (CaO) in the temperature range between – 24 and 45°C [13]. These negative activation energies are understood with reference to Equation (8). Equation 8 is rearranged if the equilibrium constant K_1 is negligibly small, $1 \gg K_1 P + K_1 K_2 P^2$:

$$\alpha \fallingdotseq \vec{k}_3 K_1 K_2 P^3 . \tag{10}$$

Thus, the apparent activation energy E' is obtained from Equation (10) as

$$E' = E - (Q_1 + Q_2)$$

here E = net activation energy of the step in Equation (3).
Q_1 = heat of adsorption of the step in Equation (1).
Q_2 = heat of adsorption of the step in Equation (7).

If the sum of Q_1 plus Q_2 is larger than E, E' becomes negative. Thus, the negative activation energy obtained by the disproportionation reaction of NO is understood in these situations. Here, the assumption that K_1 ($\equiv$[NO]/[ ]P) is negligibly small is generally used in catalytic reactions and it indicates that only a few of the active sites contribute to the reaction.

Pulse technique studies [10] of the disproportionation reaction of NO at 15°C on Y-type zeolites with various metal ions exchanged showed that alkaline earth Y-type zeolites possessed higher activities, as detailed by the activity sequence: CaY > MgY > BeY $\gg$ SrY > BaY = 0. A volcano-type relationship was found between the catalytic activity and the radius of the exchanged cation. Here, we try to explain qualitatively this relationship from the reaction rate expression of Equation (10). Equation (10) may be simplified as follows:

$$\alpha \fallingdotseq \vec{k}_3 K_1 K_2 P^3 = \vec{k}_3 K P^3 \quad (K_1 K_2 = K) . \tag{11}$$

Equation (11) shows that the reaction rate depends largely on the equilibrium constant (adsorptive power) and on the rate constant.

BeY zeolite, having the smallest ionic radius of exchanged metal, is expected to show the highest adsorptive power, whereas it possess the smallest rate constant. To the contrary, BaY-type zeolite has the largest ionic radius, and has the lowest adsorptive power, hence it is rather inactive for the disproportionation of NO.

It is easily shown that the product of K and $\vec{k}_3$, i.e., the catalytic activity, is a maximum for CaY-type zeolite, the one having the optimum adsorptive power.

3.5. INVESTIGATION FROM TPD

We discuss the TPD spectrum on the basis of the mechanistic model of Figure 4. It is reasonable to consider that the first and second peaks of the TPD spectrum, mainly composed of NO, are formed by the desorbed molecules arising from steps (2), (3), and (5) in Figure 2. However, we barely observe the IR peaks assigned to the species of step (3), because of its short lifetime [14]. Therefore, NO peaks in the TPD spectrum may be produced from the species of steps (2) and (5). In them, the NO peak of the TPD spectrum resulting from step (2) corresponds to the unreacted NO weakly adsorbed on the zeolite surface. It follows that this species desorbs at lower temperatures and becomes the first peak of the TPD spectrum. Therefore, it is understood that the first peak of the TPD spectrum has no relation to the catalytic activity, as shown in Figure 1.

On the other hand, the N_2O_3 species in the mechanistic model (5), formed by the disproportionation, are decomposed by heat and the resulting NO corresponds to the second peak of TPD. Hence the size of the second peak of the TPD spectrum varies in a similar fashion with the catalytic activity versus the pretreatment temperature, as shown in Figure 3. The maximum temperatures of the second peak of the TPD spectrum obtained on various alkaline earth Y-type zeolites were almost within the experimental error [10]. These experimental facts support the above discussion, i.e., the desorption temperature of the TPD second peak is not affected by the polarizing power of each exchanged cation, but is determined by the dissociation energy of N_2O_3 formed by the disproportionation.

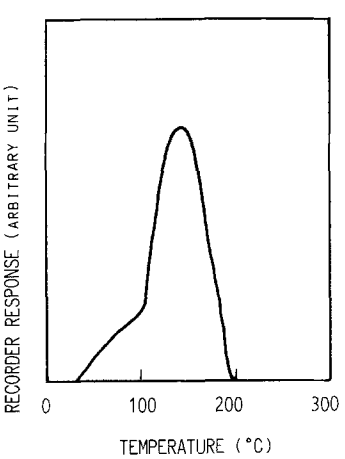

Fig. 5. Variation of N_2O content in the effluent gas of the TPD experiment.

Finally, the third peak of the TPD spectrum was mainly composed of the N_2O formed by the disproportionation, but still remaining in the zeolite structure. The remaining N_2O was confirmed by the assignment of IR spectra [14]. The variation of the amount of N_2O constituting the third peak is similar to the variation of catalytic activity, as shown in Figure 3. Hence, it may stated that the amount of the remaining N_2O increases gradually with an elevation of catalytic activity. In order to follow the movement of N_2O remaining in the zeolite structure, the effluent gas of the TPD experiment was periodically analyzed with a gas chromatograph. Figure 5 shows the variation of N_2O content, where it seems possible that two kinds of patterns exist. This indicates the possibility that N_2O produced on metal ions distributed in Site II of the faujasite structure leave the active center, and absorb onto the other sites, e.g., Si and Al sites.

References

1. J. H. Lunsford: *J. Phys. Chem.* **72**, 2141 (1968).
2. J. H. Lunsford: *J. Phys. Chem.* **72**, 4163 (1968).
3. B. M. Hoffman and N. J. Nelson: *J. Chem. Phys.* **50**, 2598 (1969).
4. C. L. Gardner and M. A. Weinberger: *Can. J. Chem.* **48**, 1317 (1970).
5. J. H. Lunsford: *J. Phys. Chem.* **74**, 1518 (1970).
6. W. E. Addison and R. M. Barrer: *J. Chem. Soc.* **70**, 757 (1955).
7. A. V. Alekseyev, V. N. Filimonov, and A. N. Terenin: *Dokl. Akad. Nauk. SSSR* **147**, 1392 (1962).
8. C. C. Chao and J. H. Lunsford: *J. Am. Chem. Soc.* **93**, 71 (1971).
9. P. H. Kasai and R. J. Bishop, Jr.: *J. Am. Chem. Soc.* **94**, 5560 (1972).
10. Y. Kanno and H. Imai: *Mater. Res. Bull.* **17**, 1161 (1982).
11. Y. Kanno and H. Imai: *Nippon Kagaku Kaishi* **1982**, 1559.
12. Y. Kanno and H. Imai: *Mater. Res. Bull.* **18**, 313 (1983).
13. Y. Kanno and H. Imai: *Chem. Lett.* **1982**, 723.
14. Y. Kanno, Y. Matsui, and H. Imai: *J. Incl. Phenom.* **3**, 461 (1985).
15. Y. Kanno and H. Imai: *Bull. Chem. Soc. Jpn.* **57**, 2046 (1984).
16. This temperature was chosen from the results obtained in reference [10]. The activity showed its maximum at a pretreatment temperature of 973 K.
17. H. Yamada, H. Kuronuma, and H. Imai: *Nippon Kagaku Kaishi* **1977**, 481.
18. J. A. Rabo, C. L. Angell, P. H. Kasai, and V. Schomaker: *Disc. Faraday. Soc.* **41**, 328 (1966).
19. C. L. Angell and P. C. Schaffer: *J. Phys. Chem.* **70**, 1413 (1966).
20. T. A. Egerton and F. S. Stone: *Trans. Faraday Soc.* **66**, 2364 (1970).
21. T. A. Egerton and F. S. Stone: *J. Chem. Soc., Faraday Trans. 1* **69**, 22 (1973).
22. The nomenclature adopted in this paper is based on that used by Breck (D. W. Breck: *Zeolite Molecular Sieves*, John Wiley, New York (1974) p. 97).
23. Y. Kanno and H. Imai: *Mater. Res. Bull.* **18**, 945 (1983).
24. J. H. Lunsford: *J. Chem. Phys.* **46**, 4347 (1967).
25. E. Wasserman, L. C. Snyder, and W. A. Tager: *J. Chem. Phys.* **44**, 1763 (1964).